SMALL-SCALE CONCENTRATING SOLAR THERMAL SYSTEM

An Undergraduate Research Scholars Thesis

by

TASNIM MOHAMED

Submitted to Honors and Undergraduate Research
Texas A&M University
in partial fulfillment of the requirements for the designation as an

UNDERGRADUATE RESEARCH SCHOLAR

Approved by
Research Advisor: Dr. Christi K. Madsen

May 2015

Major: Chemical Engineering (B.S.)

TABLE OF CONTENTS

ABSTRACT

Small-scale Concentrating Solar Thermal System. (May 2015)

Tasnim Mohamed
Department of Chemical Engineering
Texas A&M University

Research Advisor: Dr. Christi K. Madsen
Department of Electrical Engineering

In recent years, the growth of technology has caused the world energy consumption to skyrocket due to an increase in demand and an increase in available energy. Small renewable energy systems are often targeted for developing countries; however, there is a need for these systems in developed countries as well. Implementation of a renewable source of energy can reduce the level of energy poverty by providing an alternative means of obtaining energy and decreasing the cost of monthly energy bills. Currently small-scale thermal systems are commercially available for domestic hot water applications. This project tackles the problem of water heating by designing a solar concentrator that will work with and eventually replace residential water heaters. After assessing the fluid properties, a computer aided simulation to analyze the flow through the receiver for various geometries helped determine the physical design. From the flow simulations, the most reasonable internal geometry for the receiver is the single flow flat-plate design. The manufactured prototype can now be used to quantitatively model the efficiency of the receiver.

NOMENCLATURE

W	Watt
m	meter
kg	kilogram
N	Newton
K	Kelvin
GPM	gallon per minute
J	Joule
s	seond
Re	Reynold's number
D	diameter of a pipe
v	velocity of a fluid
ρ	density
μ	viscosity
f	Fanning friction factor
ΔP	pressure drop in a pipe
L	length of pipe
A	cross-sectional area
Nu	Nusselt's number
h	convective heat transfer coefficient
k	thermal conductivity
Pr	Prandtl number
$\dot{m}$	mass flow rate
c_p	heat capacity
Q	heat/thermal energy
T_s	surface temperature
T_b	bulk temperature

CHAPTER I

INTRODUCTION

In recent years, the growth of technology has caused the world energy consumption to skyrocket due to an increase in demand and an increase in available energy. The US Energy Information Administration (EIA) stated in the 2013 International Energy Outlook that the world energy consumption is projected to increase by 56% percent, from 524 quadrillion Btu to 820 quadrillion Btu, between 2010 and 2040 [1]. This raises serious concerns for the future energy supply and whether or not it can remain higher than both consumption and demand. In order to find solutions that will offset this consumption rate, an analysis must first take into account how the energy is used. For US households in particular, over 50% of the energy consumed is used for space heating and cooling based on data from 2010. The inclusion of water heating pushes this total to 72%. Thus, renewable energy systems that address heating and cooling efficiently can have a large impact on meeting a household's overall energy needs. This project tackles the problem of water heating by designing a solar concentrator that will work with and eventually replace residential water heaters.

Small renewable energy systems are often targeted for developing countries; however, there is a need for these systems in developed countries as well. One study estimates the number of US households in energy poverty at 16 million in 2005 [2]. In 2009, one in six people in rural areas fell below the US poverty line [3]. Implementation of a renewable source of energy can reduce the level of energy poverty by providing an alternative means of obtaining energy and decreasing

the cost of monthly energy bills. Currently small-scale thermal systems are commercially available for domestic hot water applications.

While the cost of photovoltaic (PV) solar panels has fallen dramatically in the last few years, other costs such as installation and maintenance start to dominate the overall system cost. In standard grid-tie systems, installation is a large fraction of the system cost in addition to the inverter and mounting hardware. For off-grid operation, energy storage by batteries increases the cost sustainability. Low-cost silicon PV panels are limited in efficiency, typically less than 20%, while thermal systems can achieve efficiencies over 50%. This is due to the fact that solar radiation is directly converted to thermal energy and eliminates the intermediary step of electrical energy conversion [4]. This project focuses on the demonstration of a stand-alone, small-scale solar thermal system. Energy storage may be achieved through a standard, commercially available hot water tank combined with an external heat exchanger.

Fresnel lenses are ideally suited for solar thermal conversion due to their light weight and fabrication from inexpensive materials such as PMMA [5, 6]. Mounted on an aluminum frame, the lens focuses the sunlight from its area of 0.774 square meters (30” by 40”) to a focal point about 33” away with an area of 1” by 3.5”. Thus, the lens greatly increases the heat flux with an estimated efficiency of 86%. Underneath the focal point lies the receiver (the evacuated tube) and the lens-to-receiver area ratio concentrates the heat flux by 67 times. The receiver is designed to absorb the concentrated light and transfer heat to the water flowing through it. Residential- and commercial-scale evacuated tube systems are currently available while solar concentrators and steam-generation plants using heliostats are currently available on an industrial

scale [7, 8]. None of these systems, however, incorporate both ideas of an evacuated tube and a concentrator. Combing both systems creates the potential for maximizing efficiency and minimizing cost.

Research was done on the materials used for currently operational evacuated tube systems. The inner heat pipe material varies in industry from copper, aluminum, or stainless steel and a compound parabolic concentrator (CPC) mirror is used to trap any diffused radiation that passes the tube. Depending on the geographic location, most residential evacuation tubes systems have a solar efficiency range of 20% to 40% [9].

CHAPTER II

METHODS

Material Properties

An important part of designing a proper heat transfer system involves choosing the right material to carry out the desired process. Thermal conductivity coefficients are important to consider for the solar thermal system design because the heat transferred from the sun's radiation must first travel through a solid medium before reaching the solar fluid. This transfer of heat involves conduction. Commercially available evacuated tube systems use copper, steel, or stainless steel for the pipe and absorber plate material.[1] Stainless steel would be more preferable than steel because stainless steel is more resistant to corrosion, so it has a higher long-term usage benefit.

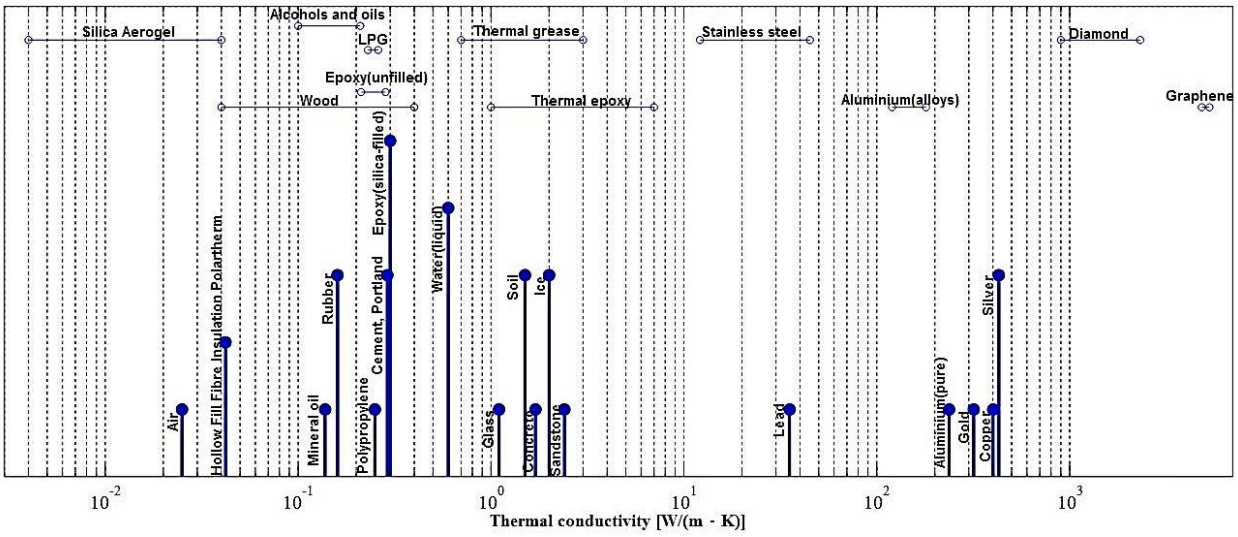

Figure 1. Experimental values of thermal conductivity

[1] Meissner, Rolf. "CPC Evacuated Tube Collector Systems for Process Heat Up to 160 °C." *Ritter XL Solar GmbH*.

According to Figure 1 above, copper has one of the largest thermal conductivity coefficients, while stainless steel is only moderately high. A high coefficient means that the heat will conduct quickly to the solar fluid; however, stainless steel is nearly half the price of copper while copper is easier to machine.[2] A simple cost-benefit analysis determined that stainless steel would be the best piping material to use inside the evacuated receiver. Also, a lower conductivity could potentially provide residual heat benefits when the radiation of the sun is no longer available, but experimental testing is still needed to prove this.

System Design

Many considerations play a role in sizing the whole system, both primary and secondary loops. The major components of the system include the Fresnel lens concentrator, the evacuated tube receiver, the plate heat exchanger, storage tanks, and DC pumps. Sizing the system takes into account the size of the tanks, the diameter of the pipes, the length of the pipes, the pressure drop across each component, etc. In order to move on to sizing the receiver, however, some values for the system must be initially determined. The following table is a list of preliminary known values and constants.

[2] http://www.onlinemetals.com/

Table 1. List of initial values and constants

heat flux	1366.1	W/m^2	
diameter of pump	0.01905	m	(3/4 in)
diameter of pipe	0.003175	m	(1/8 in)
pipe length	0.3048	m	(12 in)
density of water	1000	kg/m^3	
viscosity of water	0.001	N s/m^2	
thermal conductivity of water	0.58	W/m K	
linear expansion of stainless steel	1.60E-06	m/m K	
max volumetric flow rate	3	GPM	
	1.89E-04	m^3/s	
specific heat of water	4184	J/kg K	
desired outlet temperature	373.15	K	

The maximum flow rate is given based on the specifications of the pump. The operating flow rate is determined from the intersection of the pump and system curves. Based on the type of pump, the following graph shows the pump curve.

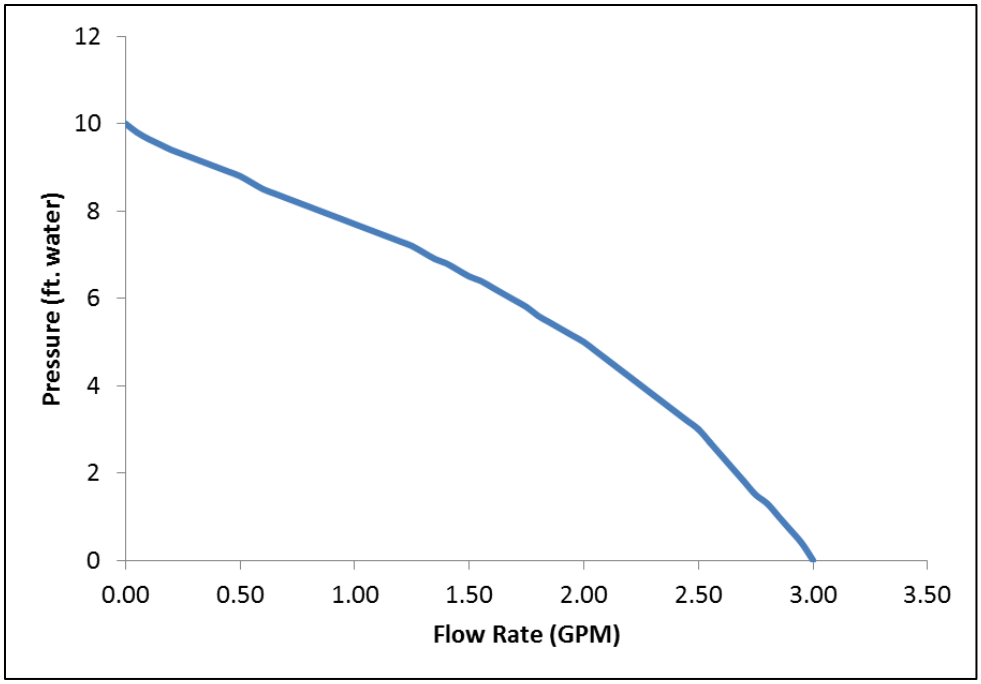

Figure 2. DC Pump Curve

To create the system curve, the flow rate was first chosen to vary between 0 and 3 GPM, then these values were converted to the SI units (in $m^3\ s^{-1}$). Using the diameter of the pipe (in m), the cross sectional area (in m^2) can be calculated to convert each flow rate to a velocity (in $m\ s^{-1}$). With this velocity, along with the pipe diameter, fluid density (in $kg\ m^{-3}$), and viscosity (in $N\ s\ m^{-2}$), the Reynolds number for each point can be calculated using Equation 1.

$$Re = \frac{Dv\rho}{\mu} \quad (1)$$

If this dimensionless number is less than 2100, then the flow is laminar. If the Re is greater than 4000, the flow is turbulent. This results in using two different empirical formulas to relate the Reynolds number to the Fanning friction factor:

$f = {}^{16}/_{Re}$ (for laminar flow)

$f = 0.079Re^{-1/4}$ (for turbulent flow).

The Fanning friction factor is defined as $f = \frac{\Delta P}{2\rho v^2}\frac{D}{L}$, so from this we can calculate the pressure drop ΔP over a length L. The pressure drop and the volumetric flow rate are converted to English units and plotted against the given pump curve for various diameters. This process was carried out for three different diameters and the corresponding graph is shown below. The point of intersection with the pump curve represents the operating flow rate of the system.

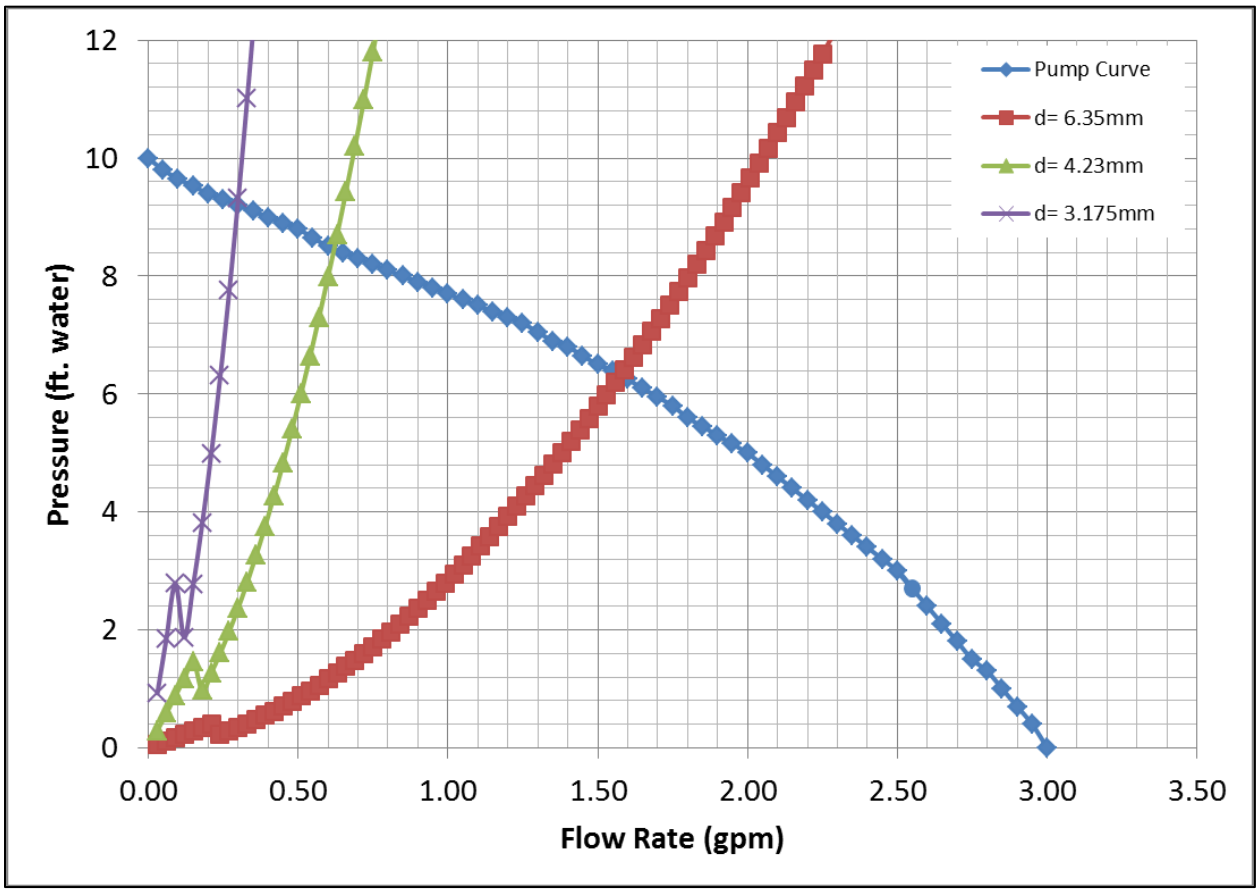

Figure 3. System curves for different diameters: (6.35mm = 1/4in, 4.23mm = 1/6in, and 3.175mm = 1/8in)

Receiver Design

Determining the operating flow rate of the whole system is useful for determining a reasonable diameter for the pipe passing through the receiver. The heat transfer performance inside the

receiver is directly determined by calculating the convective heat transfer coefficient with a series of calculations. These calculations are illustrated in the following flow diagram.

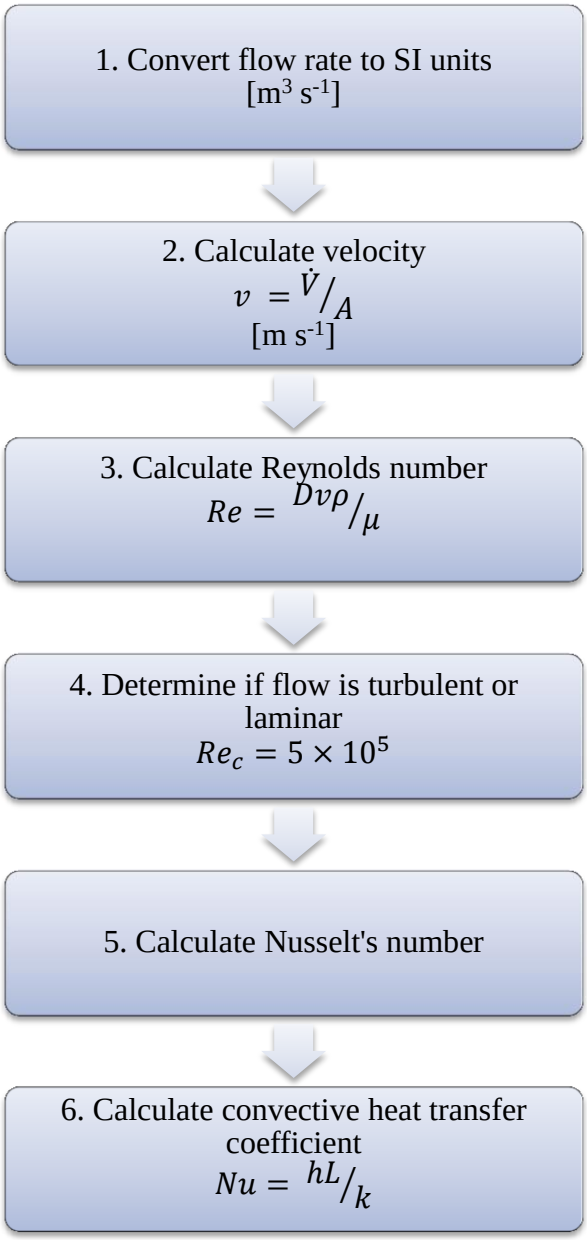

In step 4 the flow conditions are determined based on the critical Reynolds number for heat transfer, distinct from the hydrodynamic definition of turbulent and laminar flows. If $Re < Re_c$ then the flow is laminar and the Nusselt's correlation used in step 5 is simply $Nu = 48/11$ for a

constant heat flux. If $Re > Re_c$ then the flow is turbulent and Nusselt's number is calculated using the Dittus-Boelter equation (Equation 2) for forced convection.

$$Nu = 0.023 Re^{4/5} Pr^{0.4} \quad (2)$$

where Pr is the Prandtl number, $\Pr = \frac{c_p \mu}{k}$. These steps were carried out for the three diameters used in the system curve and are summarized in the following table.

Table 2. Calculated heat transfer values for three different diameters

d (mm)	**6.35**	**4.23**	**3.175**
$\dot{V}$ (GPM)	1.56	0.6	0.3
$\dot{V}$ (m^3/s)	9.84E-05	3.79E-05	1.89E-05
Velocity (m/s)	3.1078	2.6937	2.3906
Re	19734.34	11394.17	7590.13
Nu	4.36	4.36	4.36
h (w/m^2 K)	398.5683608	598.3236622	797.1367215
T_{in} (K)	369.83	364.52	355.90
T_{avg} (K)	371.49	368.84	364.52
T_s (K)	543.3042949	540.6503339	536.3376474

The inlet temperature can also be determined from the operating flow rate. An energy balance on the fluid reveals that the thermal energy absorbed by the fluid is $Q = \dot{m} c_p (T_{out} - T_{in})$. Using the fact that $\dot{m} = \rho \dot{V}$, the outlet temperature can be calculated, averaged with the inlet temperature, and used as the bulk temperature in the equation for the convective heat transfer rate: $Q = hA(T_s - T_b)$. From this, the surface temperature of the pipe wall can be calculated. Judging from these temperatures, a diameter of 6.35mm (0.25in) is the most viable dimension for the receiver because it has a minimal temperature difference and a reasonable surface temperature. A higher

temperature difference would result in a higher pressure drop, which could cause complications in the system. A surface temperature higher than the melting point of the material used for the receiver would be unreasonable.

Fluid Properties

An important consideration for heat transfer to a fluid is boiling. In this system, boiling to a vapor could cause the system to malfunction because the equipment might be specified to seal the liquid but not the vapor, so the vapors would leak out of the weaker connections. The Rohsenow correlation (Equation 3) will help to determine the ideal temperature from the heat flux.

$$\frac{q}{A} = \mu_L h_{fg} \left[\frac{g(\rho_L - \rho_v)}{\sigma}\right]^{1/2} \left[\frac{C_{pL}(T_s - T_{sat})}{C_{sf} h_{fg} Pr_L^{1.7}}\right]^3 \quad (3)$$

The ideal temperature for heat transfer is within the nucleate boiling region, as depicted in Figure 2. At this region, the heat transfer process efficiently carries away the energy created at the heat transfer surface which is desirable for this solar thermal system.

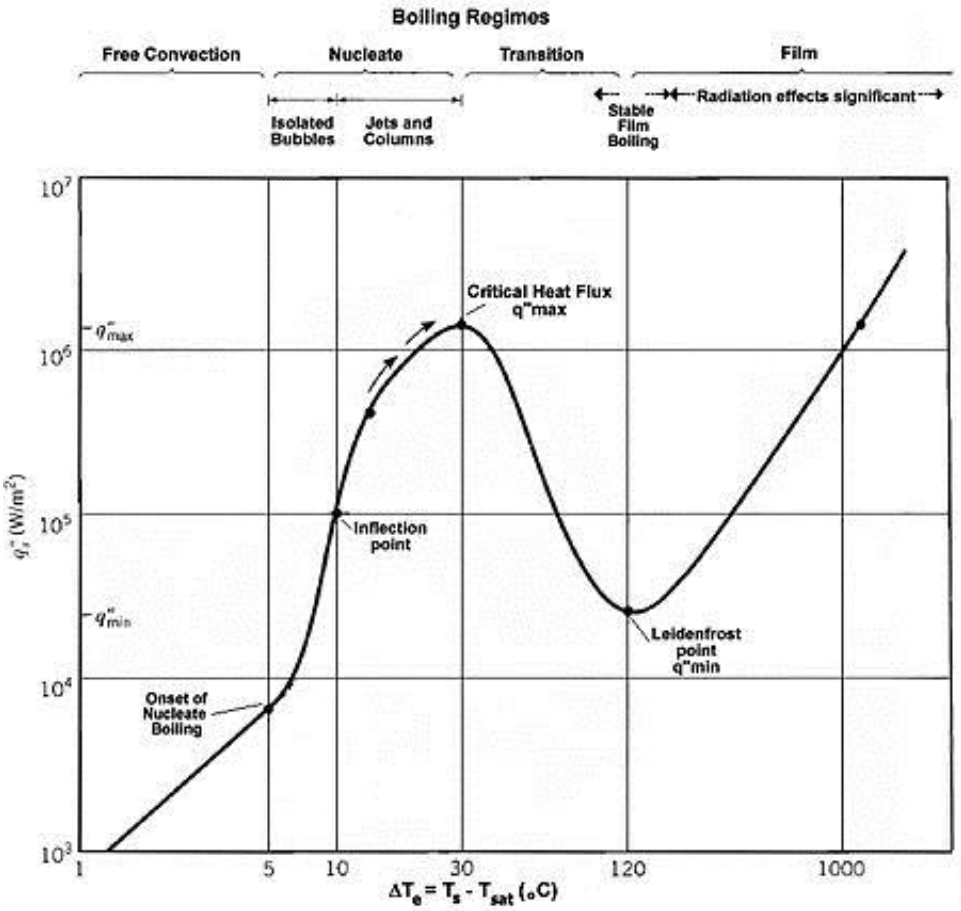

Figure 4. Boiling curve for water at 1 atm[3]

When the temperature difference is between 0°C to 10°C above T_s, the fluid is in the nucleate boiling region. Based on the calculation performed, the summarized data for the heat flux along with the temperatures are in the following table:.

Table 3. Properties of saturated water.

C_p	4217	J/kg K
h_{fg}	2257000	J/kg
ρ_L	957.9	kg/m^3
ρ_v	0.5956	kg/m^3
T_{sat}	100	°C

[3] http://en.wikipedia.org/wiki/Nucleate_boiling

Pr	1.76	
μ_L	2.79E-04	N s/m^2
σ	5.89E-02	N/m
q" max (for nucleate boiling point)	1.26E+06	w/m^2
q"s	1.37E+03	w/m^2

Table 4. Values using the Rohsenow Correlation.

Heat Flux	**T_s**	**ΔT**	
0	100.0	0.0	
17.92150207	100.5	0.5	
143.3720166	101.0	1.0	
483.8805559	101.5	1.5	
1146.976133	102.0	2.0	
1327.768245	102.1	2.1	**nucleate pool boiling**
1526.625232	102.2	2.2	

It is concluded that the heat flux for the water in the system is around 1.37x10^3 W/m^2, which is great for this experiment since we want the heat flux to be below the critical heat flux. When heat flux in the system is approaching the critical heat flux, it may change the fluid properties and might lead to damaging the components in the system (e.g. pipe, tank, etc.).

CHAPTER III

RESULTS

After assessing the fluid properties, a computer aided simulation to analyze the flow through the receiver for various geometries will help in determining the physical design. The first design is single flow through a flat-plate. The conceptual drawing is illustrated in the figure below.

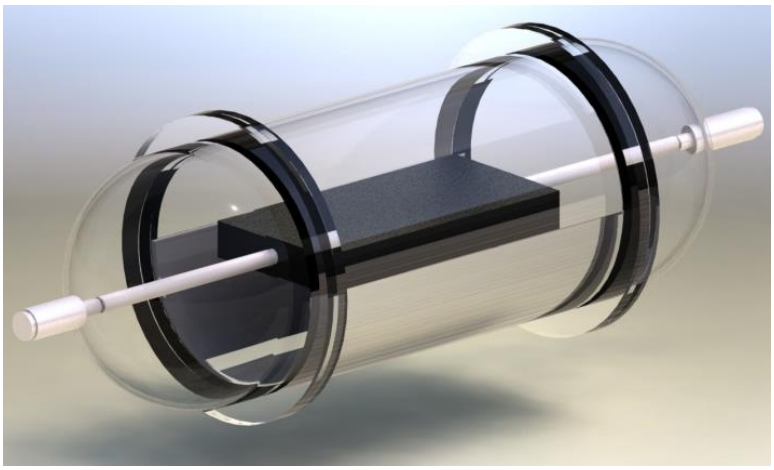

Figure 5. Flat-plate single flow

The best heat transfer will need to maximize the flow under the concentrated area of radiation in order to absorb more heat. A flow simulation provided streamlines for changes in velocity, temperature, and pressure. The figures below illustrate these three gradients for the flat-plate single flow.

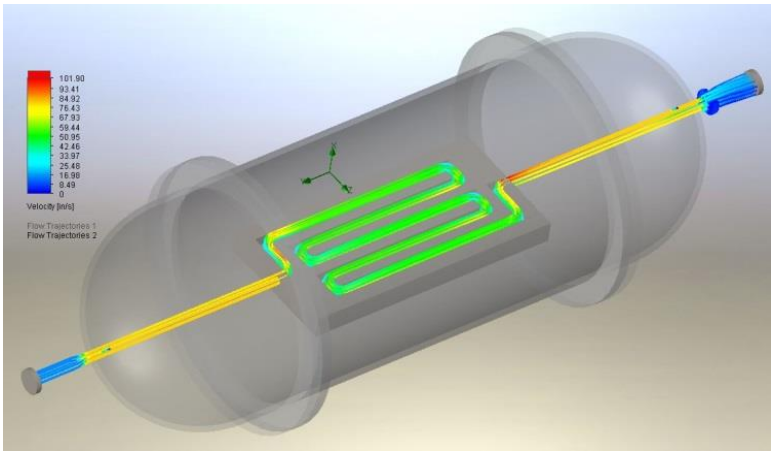

Figure 6. Velocity profile for flat-plate single flow

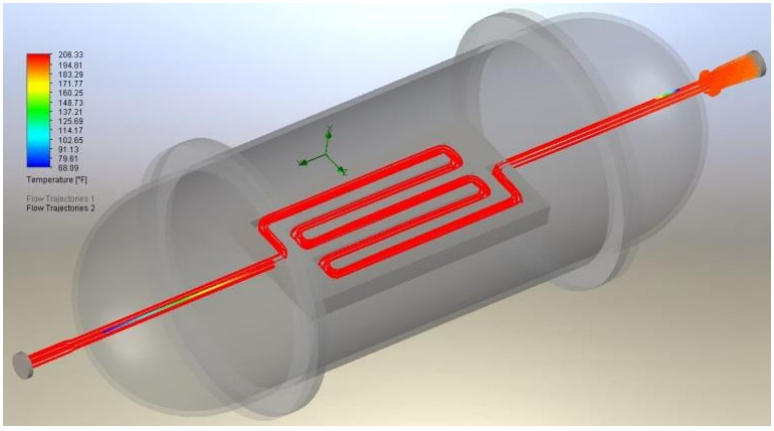

Figure 7. Temperature profile for flat-plate single flow

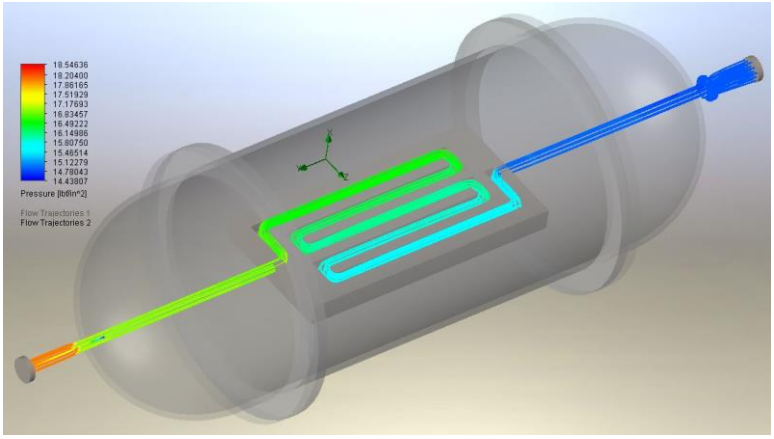

Figure 8. Pressure profile for flat-plate single flow

A second geometry was also considered. Rather than having a single flow, the flow would branch out into parallel streams. This is very similar to commercial flat-plat collectors but on a much smaller scale. The results from the parallel flow simulations are in the following figures.

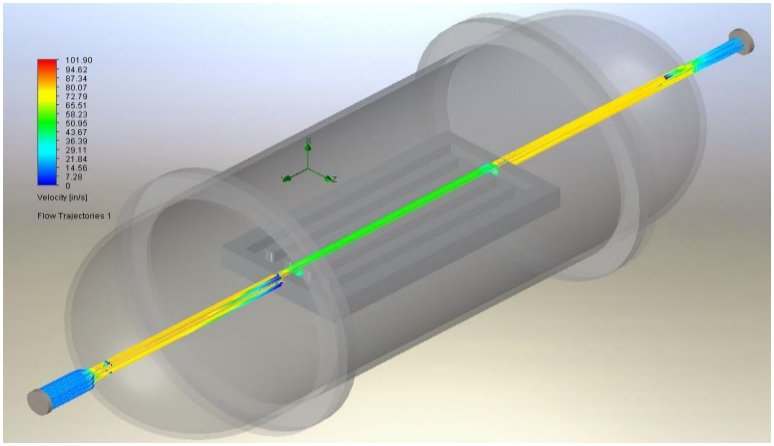

Figure 9. Velocity profile for flat-plate parallel flow

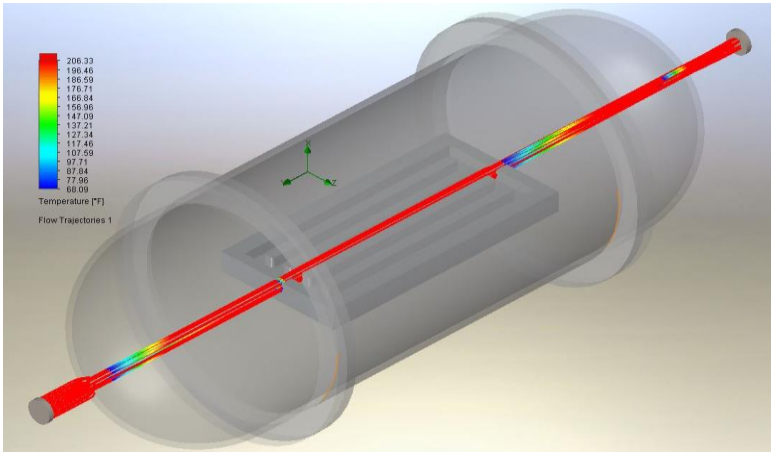

Figure 10. Temperature profile for flat-plate parallel flow

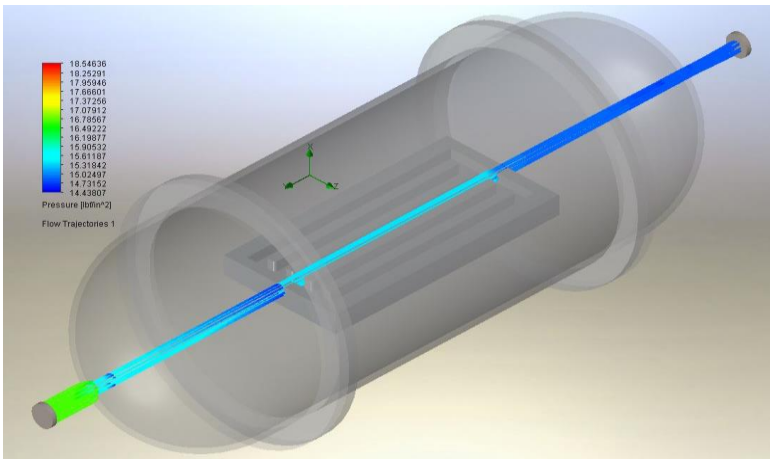

Figure 11. Pressure profile for flat-plate parallel flow

A third geometry was also considered. To increase the amount of flow underneath the heated area, a circular geometry was used. The results for this geometry are shown in the following figures.

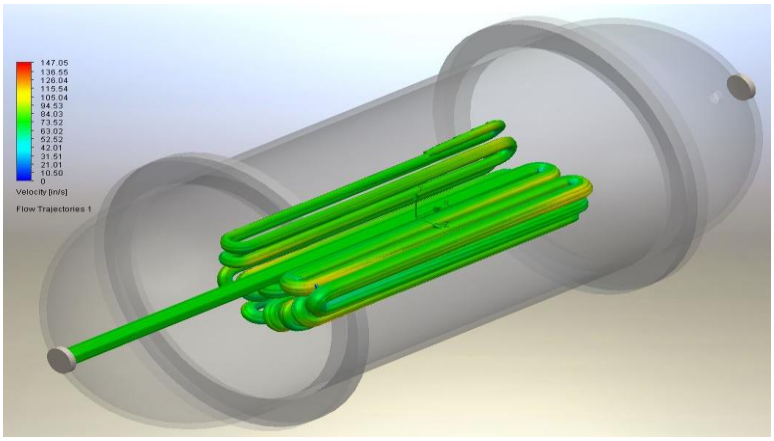

Figure 12. Velocity profile for circular flow

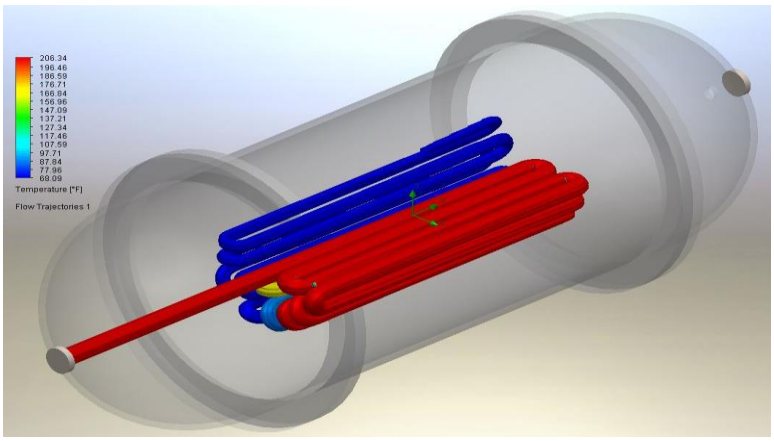

Figure 13. Temperature profile for circular flow

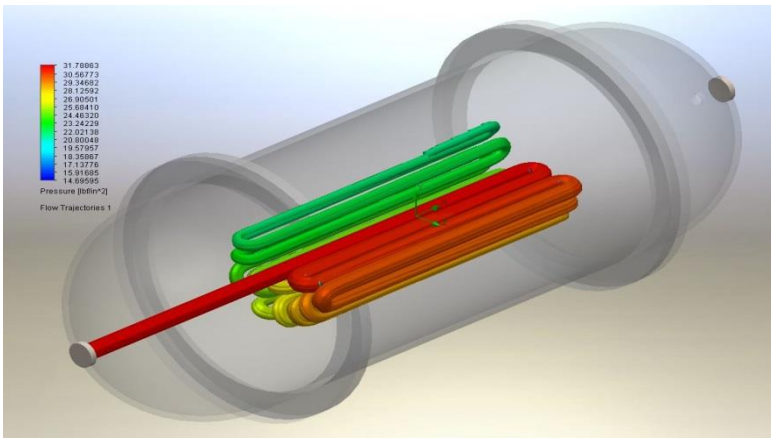

Figure 14. Pressure profile for circular flow

CHAPTER IV

CONCLUSION

From the flow simulations, the most reasonable internal geometry for the receiver is the single flow flat-plate design. By solely considering the hydrodynamics of this model, the temperature of the fluid will not decrease as it flows through the receiver. This allows for the least loss in thermal energy and a steady flow through the system. However, the simulation did not account for the radiative heat entering the system which will certainly affect the temperature gradient of the fluid flowing through the tube. This heat boundary specification was neglected in order to evaluate the sole performance of the geometry of the tubes under normal conditions.

After the determination of the internal design of the receiver, a prototype of the receiver was manufactured in the Machine Shop and the Glass Shop of the Texas A&M Department of Chemistry. With this prototype, further experiments are needed to analyze the performance and determine a quantitative model of the efficiency of the receiver. The efficiency of the receiver will be compared to a standard benchmark (a currently operating evacuated tube system) under real operating conditions.

REFERENCES

[1] “Today in Energy,” US Energy Information Administration, 2013.
Available: http://www.eia.gov/todayinenergy/detail.cfm?id=12251#

[2] M. Power, "Fuel poverty in the USA: the overview and the outlook," Energy Action, 2006.

[3] B. Bishop. (2010, 9/4/12). Poverty Highest in Rural America, Rising in Recession.
Available: http://www.dailyyonder.com/poverty-highest-rural-america-rising-recession/2010/12/21/3098

[4] E. M. Barber, Jr., “Solar thermal compared to solar electric for residential domestic water heating,” ASES Annual Conference Proceedings, 2013.
Available: http://proceedings.ases.org/wp-content/uploads/2014/02/SOLAR2013_0200_final-paper.pdf

[5] W. T. Xie, Y. J. Dai, R. Z. Wang, and K. Sumathy, "Concentrated solar energy applications using Fresnel lenses: A review," Renewable and Sustainable Energy Reviews, vol. 15, pp. 2588-2606, 2011.

[6] W. T. Xie, Y. J. Dai, and R. Z. Wang, "Numerical and experimental analysis of a point focus solar collector using high concentration imaging PMMA Fresnel lens," Energy Conversion and Management, vol. 52, pp. 2417-2426, 2011.

[7] W. Weiss and M. Rommel, “Process Heat Collectors: State of the Art within Task 33/IV,” AEE INTEC, 2008.
Available: http://aee-intec.at/0uploads/dateien560.pdf

[8] M. Newhall, “Making Solar History at Ivanpah,” US Department of Energy, 2014.
Available: http://energy.gov/articles/making-solar-power-history-ivanpah

[9] R. Meissner, “CPC evacuated tube collector systems for process heat up to 160°C,” Ritter XL Solar GmbH, 2013.
Available: http://ritter-xl-solar.com/uploads/media/Solar_process_heat_up_to_160__C__320_F_.pdf